

Mixing and CP -Violation Measurements of B^0 Mesons from the Tevatron Collider

G. Bauer

(representing the CDF and DØ Collaborations)

Massachusetts Institute of Technology, Cambridge, MA 02139, USA

E-mail: bauerg@fnal.gov

Abstract

B^0 mixing measurements from the Tevatron Run I data are reported. These include time-integrated measurements of the average mixing parameter $\bar{\chi}$, six time-dependent oscillation measurements of Δm_d , and a time-dependent limit on Δm_s . Such measurements provide constraints on CKM matrix elements. A sample of $B^0/\bar{B}^0 \rightarrow J/\psi K_S^0$ decays is used to directly measure the CP -violation parameter $\sin(2\beta)$. This value agrees well with indirect constraints on the CKM matrix.

1 B -Physics and the CKM Matrix

A major objective in the study of bottom hadrons is determining the elements of the Cabibbo-Kobayashi-Maskawa (CKM) matrix [1], and to stringently test its adequacy. This matrix transforms the flavor eigenstates of quarks into their mass eigenstates, which are not the same in the Standard Model (SM). A convenient parameterization in powers of the Cabibbo angle ($\lambda \equiv \sin \theta_C = |V_{us}|$) is due to Wolfenstein [2]:

$$V_{CKM} \equiv \begin{pmatrix} V_{ud} & V_{us} & V_{ub} \\ V_{cd} & V_{cs} & V_{cb} \\ V_{td} & V_{ts} & V_{tb} \end{pmatrix} = \begin{pmatrix} 1 - \frac{\lambda^2}{2} & \lambda & A\lambda^3(\rho - i\eta) \\ -\lambda & 1 - \frac{\lambda^2}{2} & A\lambda^2 \\ A\lambda^3(1 - \rho - i\eta) & -A\lambda^2 & 1 \end{pmatrix} + O(\lambda^4).$$

The imaginary term η was conjectured by Kobayashi and Maskawa to be the source of CP violation, which has been an outstanding issue for the last 35 years.

Constraints on the CKM matrix from the b -sector initially came from lifetime and branching ratio measurements in the early '80's. In 1986, a new window was opened by the observation of B^0 - \bar{B}^0 mixing in an unresolved mixture of B_d^0 and B_s^0 by UA1 [3] in $\bar{p}p$ collisions, and subsequently for pure B_d^0 's by ARGUS [4] at the $\Upsilon(4S)$. Through mixing, one gains access to the t CKM elements, an important consideration given the limitations of direct top studies.

Global fits to experimental data constrain the four parameters of the CKM [5, 6], with λ and A already known quite well. Constraining η and ρ has been the recent focus of B -physics. One of the unitarity constraints ($V_{tb}^*V_{td} + V_{cb}^*V_{cd} + V_{ub}^*V_{ud} = 0$), is graphically represented in Fig. 1 as a triangle in the complex ρ - η plane, with the apex at (ρ, η) . Its base is of unit length, leaving three angles and two sides that may be measured. B^0 - \bar{B}^0 mixing constrains the right leg ($\propto V_{td}/V_{ts}$), and CP violation in $B^0/\bar{B}^0 \rightarrow J/\psi K_S^0$ decays determines the angle β .

Mixing studies of B^0 mesons have greatly advanced in the '90's, and we are entering a new stage at the close of the millennium with the advent of CP -violation measurements in B^0 mesons. The contributions from the Fermilab Tevatron Collider program to these efforts from Run I (1992-6) data are discussed. The two collider experiments, CDF [7] and DØ [8], are well known, and their descriptions are not repeated here.

2 B^0 - \bar{B}^0 Mixing Measurements

2.1 B Mixing and Flavor Tagging

Like the K^0 - \bar{K}^0 system, 2nd order weak “box” diagrams result in oscillations between B^0 and \bar{B}^0 mesons. The frequency is the mass difference ($\Delta m = m_H - m_L$) between the heavy/light mass eigenstates B_H^0 and B_L^0 . The dominant effect arises from diagrams with virtual top quarks, with $\Delta m_q \sim m_t^2 F(m_t^2/m_W^2) |V_{tb}^*V_{tq}|$ for B_q^0 mesons. Thus, Δm_q constrains the CKM element relating transitions between top and the light quark q composing the B_q^0 , and relates to the right leg of the unitarity triangle (Fig. 1). The probability that an initially pure B^0 state decays as a \bar{B}^0 (and *vice versa*) at proper time t is $\mathcal{P}_{Mix}(t) = [1 - \cos(\Delta mt)]e^{-t/\tau}/2\tau$. The asymmetry between the mixed (\mathcal{P}_{Mix}) and unmixed

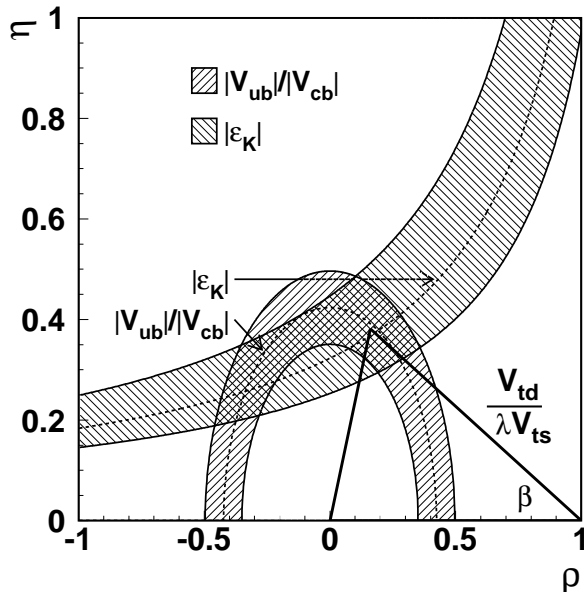


Figure 1: The CKM unitarity triangle along with constraints derived from CP violation in K^0 's (ϵ_K), and the rate of charmless B decays (V_{ub}/V_{cb}) (derived from Mele [5]). Bands indicate “ 1σ ” allowed regions. The angle $\beta = \arg(-V_{cd}V_{cb}^*/V_{td}V_{tb}^*) = \arctan(\eta/[1 - \rho])$.

(\mathcal{P}_{U_n}) states is therefore

$$\mathcal{A}_0(t) \equiv \frac{P_{U_n}(t) - P_{Mix}(t)}{P_{U_n}(t) + P_{Mix}(t)} = \cos(\Delta m_q t). \quad (1)$$

Observing B^0 mixing is predicated upon determining the b “flavor”—whether the B is composed of a b or a \bar{b} quark—at the times of production and decay. The decay flavor is usually known from the B reconstruction. More problematic is tagging the initial flavor. If this is correct with probability P_0 , then the observed asymmetry is attenuated by the “dilution” $\mathcal{D}_0 = 2P_0 - 1$, *i.e.* $\mathcal{A}_{Obs} = \mathcal{D}_0 \cos(\Delta m_q t)$. A tagger with efficiency ϵ yields an error on the asymmetry which scales as $1/\sqrt{\epsilon \mathcal{D}_0^2 N}$ for N background-free mesons, and thus $\epsilon \mathcal{D}_0^2$ measures the tagger’s effective power.

2.2 Time-Integrated Mixing Measurements

It is not necessary to measure the proper decay time to observe mixing, since

$$\chi \equiv \int_0^\infty \mathcal{P}_{Mix}(t) dt = \frac{x^2}{2(1+x^2)}, \quad \text{with } x \equiv \frac{\Delta m}{\Gamma}, \quad (2)$$

is nonzero. At the Tevatron both B_d^0 and B_s^0 are produced, and unless one explicitly identifies the B -species one measures an average $\bar{\chi} \equiv f_d\chi_d + f_s\chi_s$, for fractions f_d and f_s of the B_d^0 and B_s^0 contributions.

CDF and DØ have measured $\bar{\chi}$ using dileptons, where the leptons identify both the B and tag its flavor. Like-sign pairs indicate that one b -hadron has mixed. In 10 pb^{-1} of dimuon triggers ($p_T^\mu > 3 \text{ GeV}/c$) DØ found 59 like-sign (LS) and 113 unlike (US) pairs. The ratio $LS/US = 0.43 \pm 0.07(\text{stat.}) \pm 0.05(\text{syst.})$ is used in conjunction with models of other processes ($b \rightarrow c \rightarrow \ell^+$ sequential decays, $c\bar{c}$, fake leptons, . . . etc.) to extract $\bar{\chi} = 0.09 \pm 0.04 \pm 0.03$ [9]. Similarly, CDF has used 20 pb^{-1} of dimuons to obtain $\bar{\chi} = 0.118 \pm 0.021 \pm 0.026$ [10]; and in $e\text{-}\mu$ events $\bar{\chi} = 0.130 \pm 0.010 \pm 0.009$ [11]. All agree with $\bar{\chi} = 0.118 \pm 0.006$ from the PDG [12].

2.3 Time-Dependent B_d^0 -Mixing Measurements

With the advent of precision vertex detectors direct observation of the B_d^0 oscillation has overshadowed the $\bar{\chi}$ analyses. The DØ detector will have such tracking capability starting in Run II [13], and such studies have been restricted to CDF in Run I. Six analyses have been reported ($\sim 100 \text{ pb}^{-1}$), and are summarized in Fig. 2.

Two analyses are extensions of the time-integrated measurements described above: dilepton samples ($\sim 6000 \mu\mu$, $\sim 10000 e\mu$) are used where the leptons define both the B signal and its flavor. In this case a secondary vertex associated to a lepton is sought to establish the B -decay vertex. Average $\beta\gamma$ corrections transform the observed momentum and decay length into the proper decay time. The inclusive nature of the selection allows other processes to contribute ($c\bar{c}$, fakes, etc. . . .). Their contributions to the sample are constrained by kinematic variables, such as the relative p_T of the lepton to other parts of the decaying B . The samples are more than 80% pure $b\bar{b}$. The oscillation is revealed in the time variation of the like-sign dilepton fraction, and fits extract Δm_d (see “ μ/μ ” [14] and “ e/μ ” in Fig. 2).

In another dilepton analysis [15] the B_d^0 is more cleanly identified by reconstructing a D^* near a lepton. From the lepton on the other side one infers the initial flavor of the $B \rightarrow \ell^+ D^{*-} X$ meson. The oscillation from a signal of ~ 500 events is shown in Fig. 2 under “ $D^*\text{lep/lep}$,” along with its Δm_d . The

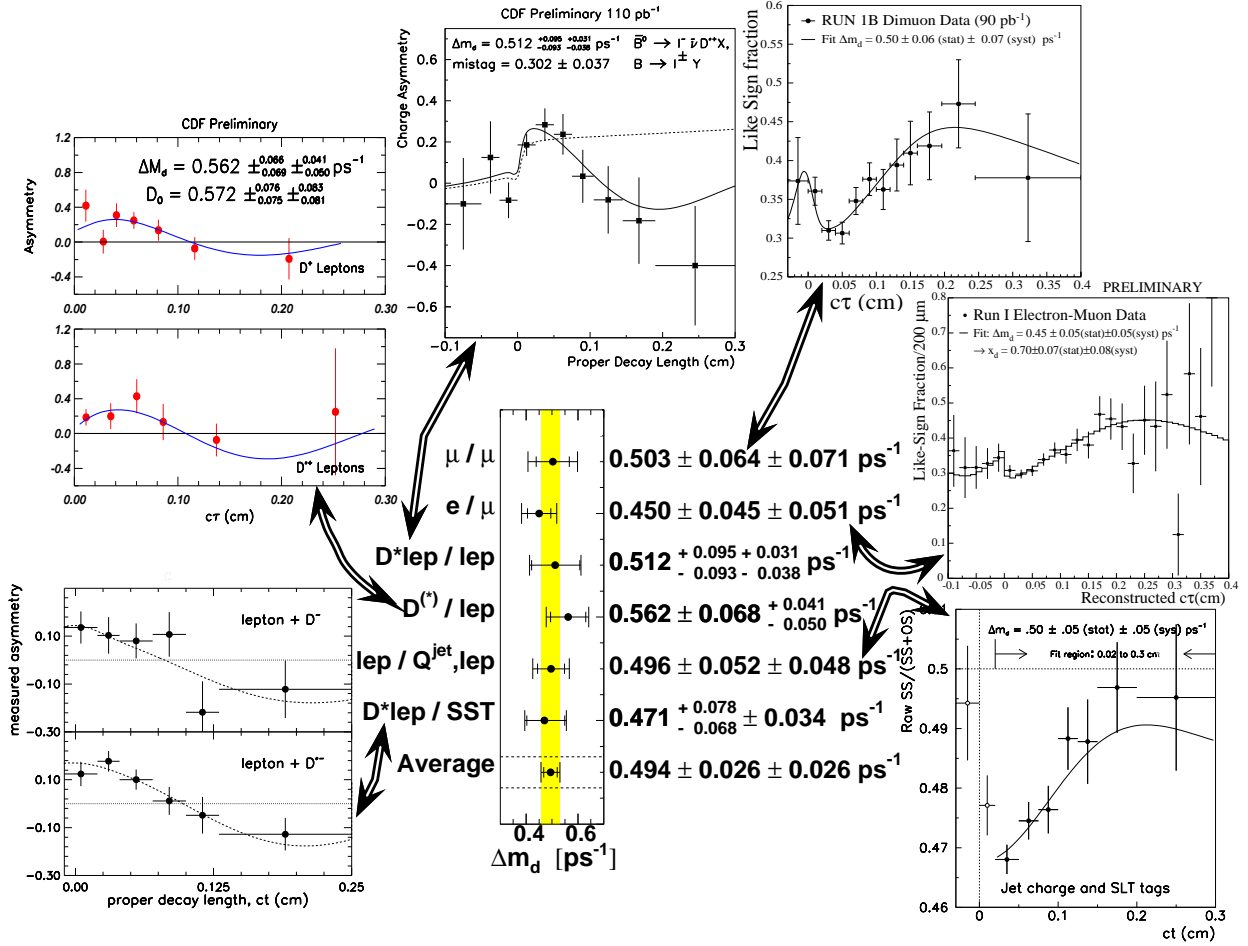


Figure 2: Summary of the six CDF B_d^0 oscillation measurements of Δm_d . In each case an oscillation is observed in a charge-correlation asymmetry as a function of proper decay length. The average CDF Δm_d accounts for correlations between measurements.

cleanliness of the sample results in a small systematic error ($^{+0.31}_{-0.38}$), but at the price of worse statistical precision.

Inclusive lepton triggers (e and μ , $p_T > 8 \text{ GeV}/c$) are used to obtain a tagged B sample, where the B flavor on the opposite side is identified by reconstructing a $D^{(*)-}$. The resulting oscillation for ~ 800 events is labeled as “ $D^{(*)}/\text{lep}$ ” in Fig. 2 [16].

We next consider the “ $\text{lep}/Q^{\text{jet}},\text{lep}$ ” analysis [17], which again uses a lepton+vertex to identify a b -hadron and a second lepton as a tag. It also uses the subtle technique of “jet-charge” tagging. The sample arises from inclusive

lepton triggers, where we search for another lepton as a tag similar to the earlier analyses. We do not dwell on this aspect. More interesting is the use of “jet-charge” tagging, where an average charge of a jet opposite the ℓ +vertex is used to infer the initial flavor of the b -hadron producing the trigger lepton. The charge of the away-side jet is defined as

$$Q_{jet} \equiv \frac{\sum_i q_i (\vec{p}_i \cdot \hat{a})}{\sum_i \vec{p}_i \cdot \hat{a}}, \quad (3)$$

where q_i and \vec{p}_i are the charge and momentum of the i -th track in the jet, and \hat{a} is the unit vector pointing along the jet axis. A negative (positive) Q_{jet} implies the jet contained a b (\bar{b}). One finds that the tag purity is higher for larger $|Q_{jet}|$. The sample composition is again determined via kinematic variables like the p_T^{rel} of the trigger lepton and the invariant mass of the secondary vertex. The fit results of the tagging asymmetry for $\sim \frac{1}{4}$ million events are given in Fig. 2 as “lep/ Q^{jet} lep.”

The sixth analysis uses “Same-Side Tagging” (SST), where a track near the reconstructed B tags its flavor [18], rather than using the other b -hadron. The idea is simple. A \bar{b} quark hadronizing into a B_d^0 picks up a d in the fragmentation, leaving a \bar{d} . To make a charged pion, the \bar{d} picks up a u making a π^+ . Conversely, a \bar{B}_d^0 will be associated with a π^- . Correlated pions also arise from $B^{**+} \rightarrow B^{(*)0} \pi^+$ decays. Both sources have the same correlation, and are not distinguished here.¹

CDF adopted a “ p_T^{rel} ” algorithm, where the tag is the candidate track with the smallest momentum component transverse to the B +Track momentum. A charged particle is a valid SST candidate if it is reconstructed in the Si- μ vertex detector (SVX), has $p_T > 400$ MeV/ c , is within $\Delta R = \sqrt{(\Delta\eta)^2 + (\Delta\phi)^2} \leq 0.7$ of the B , and its impact parameter is within 3σ of the primary vertex.

SST is applied to almost 10,000 $B \rightarrow \ell^+ D^{(*)} X$ events reconstructed via four B_d^0 decay signatures and one for B^+ [20, 21]. The sample composition is unraveled in the fit (including $B_d^0 \leftrightarrow B^+$ cross-talk). The χ^2 fit results are shown in Fig. 2 as “ D^* lep/SST,” with the upper plot showing the $B_d^0 \rightarrow \ell^+ D^- X$ reconstruction and the lower one is for $\ell^+ \bar{D}^{*-} X$. Along with Δm_d , one also

¹ A recent CDF B^{**} analysis of a $\ell D^{(*)}$ sample found the fraction of B mesons arising from B^{**} states to be $0.28 \pm 0.06 \pm 0.03$ [19]. B^{**} mesons are indeed a significant source of correlated pions.

obtains the dilution, $\mathcal{D}_0 = 0.181_{-0.032}^{+0.036}$, of this SST method. This analysis provides the dilution calibration for the SST analyses of Sec. 3.

The six Δm_d results are combined, accounting for correlations, into a CDF average of $0.481 \pm 0.026 \pm 0.026 \text{ ps}^{-1}$. This is comparable to other experiments, and is in good agreement with the PDG value of $0.464 \pm 0.018 \text{ ps}^{-1}$ [12].

2.4 Time-Dependent B_s^0 -Mixing Measurements

B_s^0 mixing follows the same formalism as for B_d^0 's, except the relevant CKM element is V_{ts} rather than V_{td} . Measurements of $\bar{\chi}$ (Sec 2.2), along with χ_d measured at the $\Upsilon(4S)$ and estimates for the species fractions f_d and f_s , provided the original direct indication that χ_s is close to its asymptotic limit (1/2) and thereby insensitive to Δm_s . Further progress on B_s^0 mixing necessitates time-dependent methods.

CDF has searched for B_s^0 oscillations [22] using dileptons (110 pb^{-1} of $\mu\mu$ or $e\mu$) for $\ell^\pm \ell^\mp \phi h^-$, where h^- is a charged track associated to a $\phi \rightarrow K^+ K^-$ decay vertex. This signature selects $B_s^0 \rightarrow \ell^+ \nu D_s^-$, $D_s^- \rightarrow \phi \pi^- X$; exclusive reconstruction is not required to increase statistics. The resulting $K^+ K^-$ mass distribution is shown in Fig. 3. The B_s^0 decay point is obtained by projecting the ϕh^- decay back to the ℓ^+ . Monte Carlo corrections are applied to the $\beta\gamma$ factor for the proper time estimation. A sample of $1068 \pm 70 B_s^0$ candidates (purity of $61.0_{-7.0}^{+4.4}\%$) is obtained.

The B_s^0 flavor is inferred from the other trigger lepton, similar to the Δm_d analyses. Events are again classified as “unmixed” ($\ell^\pm \ell_{tag}^\mp$) or “mixed” ($\ell^\pm \ell_{tag}^\pm$). Limits will be set rather than an observation of the oscillation, so one must know *a priori* the mistag rate R_m . This was found to be $R_m = \frac{1}{2}(1 - \mathcal{D}_0) = 0.24 \pm 0.08$ from a likelihood fit of the mixed/unmixed fractions in the $\ell^+ \phi$ data. The B_s^0 oscillation is too rapid to influence the determination of R_m ; rather it is governed by the sample contributions of B_d^0 , B^+ , $c\bar{c}$, sequential decays and fake background.

The data are fit with an unbinned likelihood to describe the mixed versus unmixed components. The fit includes the various sources of events (B_s^0 , B_d^0 , B^+ , ...) and Δm_s is a free parameter. No oscillation is observed, and limits are set. The amplitude method [23] is adopted, whereby the functional form of $\cos(\Delta m_s t)$ is replaced by $A(\Delta m_s) \cos(\Delta m_s t)$, *i.e.* the amplitude is a free Δm_s -

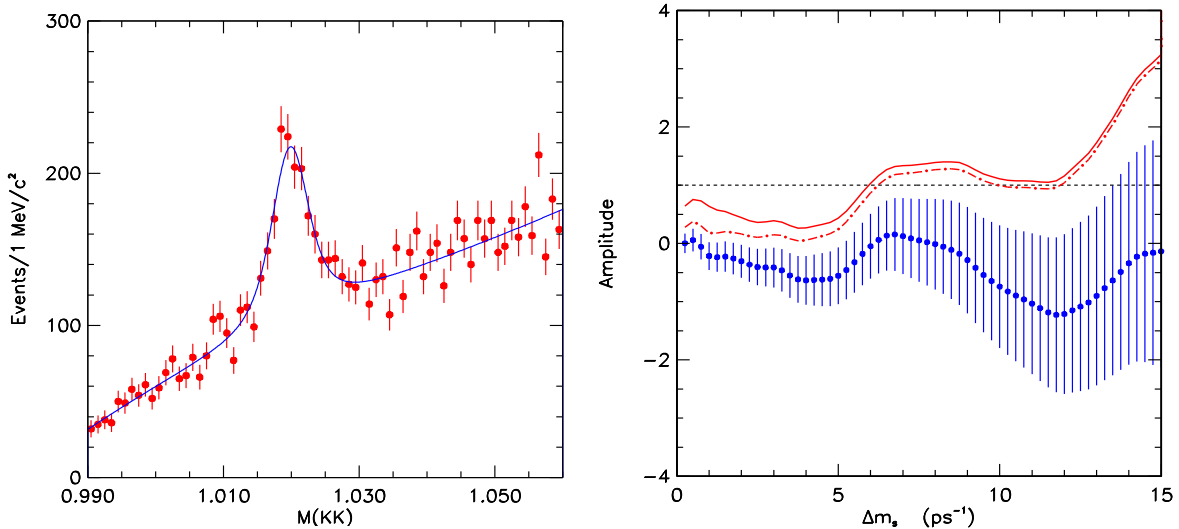


Figure 3: Left: The K^+K^- mass distribution showing the ϕ peak. Right: The likelihood amplitude scan through Δm_s (points), and the 95% CL limits on the amplitude for statistical error (dashed curve) and statistical and systematic errors combined (solid curve).

dependent parameter. For the true value Δm_s^{true} , $A(\Delta m_s^{true}) = 1$, and otherwise $A(\Delta m_s) = 0$. The result of the scan of $A(\Delta m_s)$ from the likelihood is shown in Fig. 3. The data fluctuate about zero, with no evidence for an oscillation. Values of Δm_s are excluded at the 95% CL if $A(\Delta m_s) + 1.645\sigma_A(\Delta m_s) \leq 1$, and thus $\Delta m_s > 5.8 \text{ ps}^{-1}$ at 95% CL accounting for both statistical and systematic errors (Fig. 3, solid line).

This result is competitive with other single tagging measurements. However, the world limit, $\Delta m_s > 12.4 \text{ ps}^{-1}$ (95% CL), is dominated by the multi-tag results from ALEPH and DELPHI [24].

It is conceivable that B_s^0 oscillations are too rapid to be directly observed. If so, the width difference $\Delta\Gamma_s$ between the mass eigenstates is expected to be large. CDF has searched for two lifetime components in a ℓD_s sample, and finds $\Delta\Gamma_s/\Gamma_s < 0.83$ at 95% CL [25]. Given $\Delta\Gamma_s/\Delta m_s$ and the mean B_s^0 lifetime $\bar{\tau}_s$, this can be expressed as the upper bound $\Delta m_s < 96 \text{ ps}^{-1} \times [5.6 \times 10^{-3}/(\Delta\Gamma_s/\Delta m_s)][1.55\text{ps}/\bar{\tau}_s]$ at 95% CL., with $\Delta\Gamma_s/\Delta m_s = 5.6 \times 10^{-3}$ a recent estimate [26]. The limit is weak, but with the increased statistics of Run II either Δm_s or $\Delta\Gamma_s$ should be directly determined.

3 CP Violation in $J/\psi K_S^0$

The origin of CP violation has been an outstanding question since its unexpected discovery in $K_L^0 \rightarrow \pi^+\pi^-$ 35 years ago [27]. In 1972, before the discovery of charm, Kobayashi and Maskawa [1] proposed that this was the result of quark mixing with 3 (or more) generations. Unfortunately the K^0 has been the only place CP violation has been observed. Despite precision K^0 -studies, a complete picture of CP violation is still lacking; and it is often argued that the CKM model can *not* be the full story [28].

CP -violation searches have encompassed B mesons, but the effects in inclusive studies [10, 29] are too small ($\sim 10^{-3}$) to as yet detect. In the early '80's it was realized [30] that the mixing *interference* of B_d^0 decays into the same CP state could manifest large violations. Unfortunately these decays were, until recently, too rare to study.

The “golden” mode for observing large CP violation in B 's is $B_d^0/\bar{B}_d^0 \rightarrow J/\psi K_S^0$,² and, critically, it is related to the CKM matrix with little theoretical uncertainty. A B_d^0 may decay directly to $J/\psi K_S^0$, or the B_d^0 may oscillate into \bar{B}_d^0 and then decay to $J/\psi K_S^0$. These two paths have a phase difference, quantified by the angle β of the unitarity triangle (Fig. 1). This gives rise to a decay asymmetry

$$\mathcal{A}_{CP}(t) \equiv \frac{\bar{B}_d^0(t) - B_d^0(t)}{\bar{B}_d^0(t) + B_d^0(t)} = \sin(2\beta) \sin(\Delta m_d t), \quad (4)$$

where $B_d^0(t)$ [$\bar{B}_d^0(t)$] is the number of decays to $J/\psi K_S^0$ at proper time t given that the meson was a B_d^0 [\bar{B}_d^0] at $t = 0$. OPAL investigated CP violation with 24 $J/\psi K_S^0$ candidates (60% purity), and obtained $\sin(2\beta) = 3.2_{-2.0}^{+1.8} \pm 0.5$ [32]. CDF has taken advantage of the large B cross section at the Tevatron and obtained a sample of several hundred decays to $J/\psi K_S^0$ to measure $\sin(2\beta)$ [33].

² Another mode of possible interest is $B_d^0 \rightarrow J/\psi K^{*0}$. While this is not a CP eigenstate, it can be decomposed into even and odd eigenstates by an angular analysis. This has been done by CDF for $B_d^0 \rightarrow J/\psi K^{*0}$ (and $B_s^0 \rightarrow J/\psi \phi$) to extract the decay matrix elements [31], but the Run I statistics are insufficient to be of interest for measuring CP -violation parameters.

3.1 Same Side Tagging Analysis of $J/\psi K_S^0$

$J/\psi K_S^0$ candidates are selected from the $J/\psi \rightarrow \mu^+\mu^-$ sample (110 pb^{-1}). A time-dependent analysis demands that both muons are in the Si- μ vertex detector (SVX), cutting away half of the J/ψ 's. The $K_S^0 \rightarrow \pi^+\pi^-$ reconstruction tries all tracks, assumed to be pions. The $p_T(K_S^0)$ must be above $0.7 \text{ GeV}/c$, its decay vertex displaced from the J/ψ 's by more than 5σ , and $p_T(B_d^0) > 4.5 \text{ GeV}/c$. We construct $M_N \equiv (M_{FIT} - M_0)/\sigma_{FIT}$, where M_{FIT} is the fitted $J/\psi K_S^0$ mass, σ_{FIT} its error ($\sim 9 \text{ MeV}/c^2$), and M_0 is the central B_d^0 mass. The distribution for candidates with $ct > 0$ is shown in Fig. 4a. A likelihood fit yields (for all ct) $198 \pm 17 B_d^0/\bar{B}_d^0$'s.

The initial flavor is tagged by the identical SST of the $\ell D^{(*)} \Delta m_d$ measurement of Sec. 2.3. SST is independent of the B_d^0 decay mode, and therefore the dilution measurement can be transferred from one mode to another. However a small kinematic correction, determined from Monte Carlo, is made to translate the $\ell D^{(*)}$ dilution to the $J/\psi K_S^0$ sample due to the different $p_T(B)$ ranges [21]. The appropriate \mathcal{D}_0 is $0.166 \pm 0.018 \pm 0.013$ [33], where the first error is due to the dilution measurements, and the second is due to the translation to the $J/\psi K_S^0$ sample.

The SST method is applied to the $J/\psi K_S^0$ sample, with a resultant tagging efficiency of $\sim 65\%$. Analogous to Eq. (4), we compute the asymmetry

$$\mathcal{A}(ct) \equiv \frac{N^-(ct) - N^+(ct)}{N^-(ct) + N^+(ct)}, \quad (5)$$

where $N^\pm(ct)$ are the numbers of positive and negative tags (implying B_d^0 and \bar{B}_d^0 respectively) in a given ct -bin. Signal and sideband regions are defined as $|M_N| < 3$ and $3 < |M_N| < 20$, and the sideband-subtracted asymmetry of Eq. (5) is plotted in Fig. 4c. The dashed curve is a χ^2 fit of $\mathcal{D}_0 \sin(2\beta) \sin(\Delta m_d t)$ to the data, with Δm_d fixed to 0.474 ps^{-1} [34]. The amplitude, 0.36 ± 0.19 , measures $\sin(2\beta)$ attenuated by the dilution \mathcal{D}_0 . Due to the $\sin(\Delta m_d t)$ shape the fit amplitude is driven by the asymmetries at larger ct 's, where backgrounds are small (see Fig. 4b).

The fit is refined using an unbinned likelihood fit. This makes optimal use of the low statistics by fitting the data in M_N and ct , including sideband and $ct < 0$ events which help constrain the background. The fit also incorporates resolutions and corrections for (small) systematic detector biases. The solid curves in

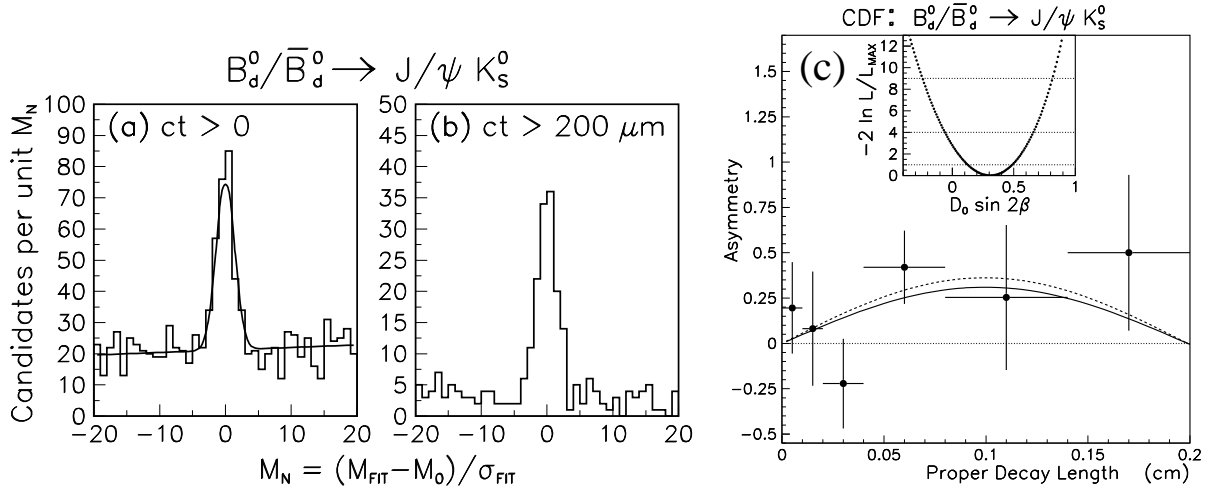


Figure 4: The normalized mass distribution of $J/\psi K_S^0$ events with $ct > 0$ (a) and $200 \mu\text{m}$ (b). The curve is the Gaussian signal plus linear background from the likelihood fit (see text). The sideband-subtracted flavor asymmetry (c) as a function of the $J/\psi K_S^0$ proper decay length [Eq. (5)]: points are data, dashed curve is a simple χ^2 fit, and the solid curve is the likelihood fit. The inset shows a scan of the log-likelihood function as $\mathcal{D}_0 \sin(2\beta)$ is varied about the best fit value.

Fig. 4a,c are the result of the likelihood fit, which gives $\mathcal{D}_0 \sin(2\beta) = 0.31 \pm 0.18$. As expected, both fits give similar values since the result is dominated by the sample size. The systematic uncertainty on $\mathcal{D}_0 \sin(2\beta)$ is 0.03, dominated by the uncertainty on Δm_d ($\pm 0.031 \text{ ps}^{-1}$), but includes the effects from detector biases and the B_d^0 lifetime.

To extract $\sin(2\beta)$ from the measured asymmetry the dilution must be divided out. However, as long as $\mathcal{D}_0 \neq 0$, the exclusion of $\sin(2\beta) = 0$ is *independent* of further knowledge of \mathcal{D}_0 . Given $\mathcal{D}_0 > 0$, the unified frequentist approach of Feldman and Cousins [35] yields a dilution-independent exclusion of $\sin(2\beta) \leq 0$ at 90% CL.

From above, $\mathcal{D}_0 = 0.166 \pm 0.018 \pm 0.013$, which results in $\sin(2\beta) = 1.8 \pm 1.1 \pm 0.3$. The central value is unphysical since the amplitude of the raw asymmetry is larger than \mathcal{D}_0 . This result corresponds to excluding $\sin(2\beta) < -0.20$ at a 95% CL.

3.2 Multi-Tagging Analysis of $J/\psi K_S^0$

Shortly after this conference CDF released an expanded $J/\psi K_S^0$ analysis using three taggers, as well as non-SVX data. These preliminary results are briefly summarized.

The above SST result is statistically very limited. It can be improved by increasing the *effective* statistics by using lepton and jet-charge tagging to increase the total $\epsilon \mathcal{D}_0^2$. The raw statistics can also be increased by utilizing the J/ψ candidates not reconstructed in the SVX. Precision lifetime information is lost, reducing the power of these events, but significant information remains. The $J/\psi K_S^0$ selection is otherwise similar to the SST-only analysis, and results in a total of 395 ± 31 $J/\psi K_S^0$ candidates (202 ± 18 in the SVX, 193 ± 26 are non-SVX).

SST, lepton, and jet-charge tagging are applied to this sample. Lepton tagging follows the Δm_d analyses. The jet-charge algorithm is similar to the Δm_d analysis but uses a “mass” jet algorithm rather than a “cone” based one. This improves the efficiency for identifying low- p_T “jets” for the tag. A lepton tends to dominate the jet charge if a lepton tag is in the jet. Since lepton tagging has low efficiency but high dilution, the correlation between lepton and jet-charge tags is avoided by dropping the jet-charge tag if there is a lepton tag. The dilutions of these two methods are measured in $B^+ \rightarrow J/\psi K^+$ decays (Table 1), and are directly applicable to the $J/\psi K_S^0$ sample. The precision is not high, but this obviates the complex problem of translating dilutions from kinematically different samples.

The tagged $J/\psi K_S^0$ events are fit in an unbinned likelihood fit (Δm_d constrained to 0.464 ± 0.018 ps⁻¹ [12]). The $\sin(2\beta)$ results for the individually tagged subsamples are listed in Table 1, including systematic errors due to the dilutions, Δm_d , τ_{B^0} , and m_{B^0} . The SST result is slightly larger than before with the inclusion of the non-SVX events, and the error has decreased by $\sim 20\%$. The other two taggers fall in the physical range, one positive and the other negative.

Rather than average these three results, the likelihood fitter is generalized to fit all three simultaneously while accounting for tag correlations. The global multi-tag result is $\sin(2\beta) = 0.79_{-0.44}^{+0.41}$ (Fig. 5), including the systematic uncertainties. This result corresponds to a unified frequentist confidence interval of $0.0 < \sin(2\beta) < 1$ at 93% CL. Although the exclusion of zero has only slightly

Table 1: Multi-tag analysis of $J/\psi K_s^0$. There are two dilutions for SST, one for SVX events and another for non-SVX events.

| Tagger | Eff. (%) | Dil. (%) | $\sin(2\beta)$ |
|--------------------|---------------------------------------|-----------------|-------------------------|
| SST _{svx} | 35.5 ± 3.7 | 16.6 ± 2.2 | $2.03^{+0.84}_{-0.77}$ |
| SST _{non} | 38.1 ± 3.9 | 17.4 ± 3.6 | $0.52^{+0.61}_{-0.75}$ |
| Lepton | 5.6 ± 1.8 | 62.5 ± 14.6 | $-0.31^{+0.81}_{-0.85}$ |
| Jet- Q | 40.2 ± 3.9 | 23.5 ± 6.9 | $0.79^{+0.41}_{-0.44}$ |
| Global | $\epsilon\mathcal{D}^2 = 6.3 \pm 1.7$ | | |

increased from 90% for the (SVX) SST-only analysis, the uncertainty on $\sin(2\beta)$ is cut in half.

4 Summary and Prospects

Measurements of Δm_d and Δm_s provide important constraints on the CKM matrix. World averages constrain the triangle of Fig. 1 quite well, as shown in Fig. 6. An indirect determination of $\sin(2\beta) = 0.77^{+0.09}_{-0.12}$ was reported at this conference [6]. This is much more precise than the direct CDF measurement; nevertheless, the agreement is an auspicious omen for the CKM model's account of CP violation.

Additional sources of CP violation are, however, thought necessary to account for the baryon asymmetry in the universe [28]. Searching for physics beyond the CKM model demands stringent tests, and is the focus of dedicated B factories. Both CDF and DØ will also be fully engaged in this effort by exploiting the rich B harvest from Run II. Commencing in 2000, a two-year run will deliver $20\times$ the luminosity ($\sim 2 \text{ fb}^{-1}$), to be exploited by greatly enhanced detectors. With the “baseline” detector and trigger upgrades [13, 36] CDF projects 10,000 $J/\psi K_s^0$ dimuon triggers for a $\sin(2\beta)$ error of about ± 0.08 ; and DØ, with a new precision tracking system, expects an error of 0.12-0.15 (Fig. 6). Dielectron triggers may further increase the samples by $\sim 50\%$. These errors are in the range projected for B factories. The Run II Tevatron will be competitive in many other areas of B_d^0 physics as well.

B_s^0 oscillations have, so far, eluded all comers. The Tevatron should have a

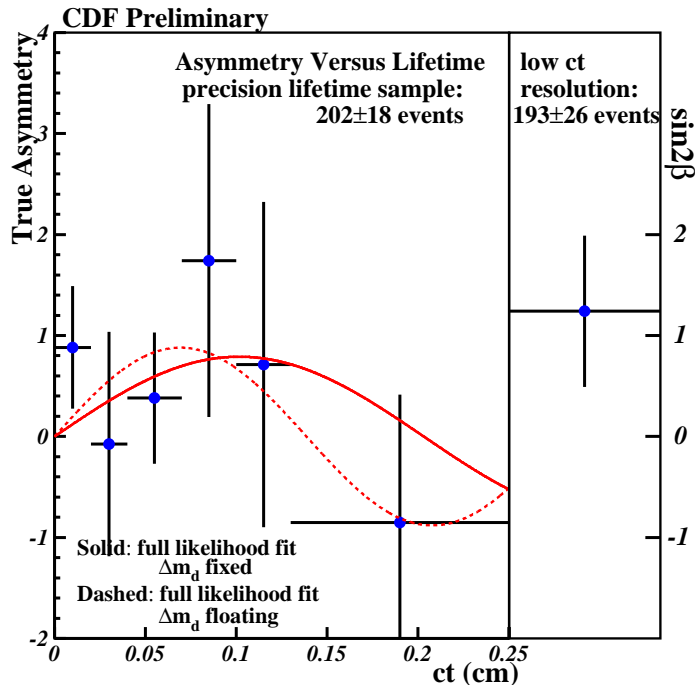


Figure 5: Multi-tag $\sin(2\beta)$ result. Left: time-dependent asymmetry of SVX data; Right: time-integrated asymmetry of non-SVX data.

virtual monopoly on the B_s^0 after the closure of the Z^0 machines and before the start of the LHC. Run II baseline expectations are for CDF to reach x_s 's up to 30-40, and DØ up to 20-25. Although DØ's reach is less, it is sufficient that failure to observe oscillations should critically challenge the CKM model.

In addition to the baseline upgrades, both experiments are aggressively pursuing further improvements. For example, CDF is working towards an additional Si-layer to improve vertex resolution and a Time-of-Flight system, which may push x_s out to ~ 60 ; and DØ is looking at a displaced-track trigger to greatly enhance B triggering.

We close with the CKM model unscathed, but look forward to an exciting future where, perhaps, some of the mystery surrounding CP violation may be unveiled.

Acknowledgments

I would like to thank my fellow collaborators, and colleagues across the ring, for the pleasure of representing them and their work. Assistance with this

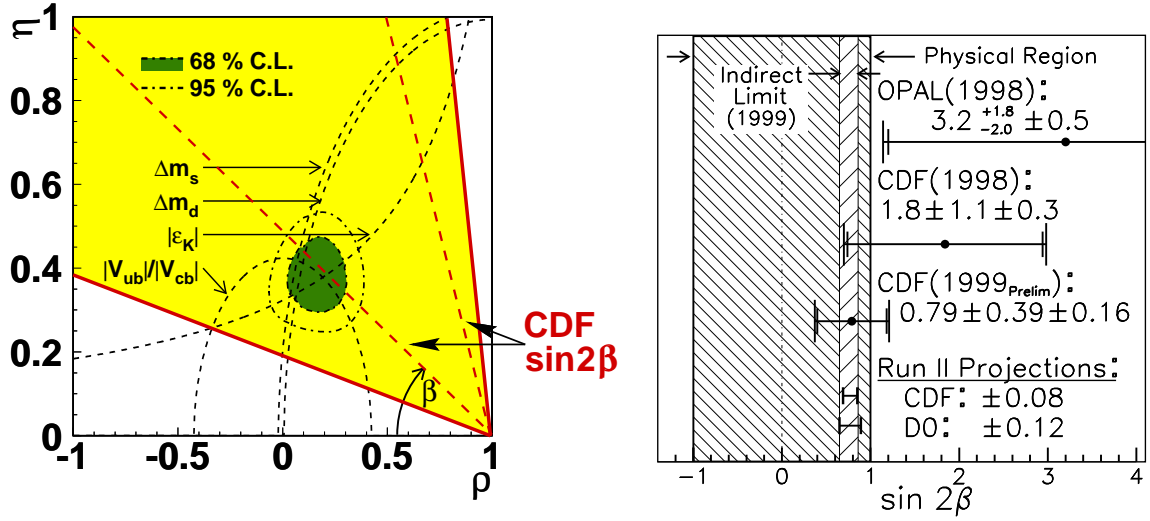


Figure 6: Left: CKM constraints from K_L^0 's, charmless B decays, Δm_d , and Δm_s on (ρ, η) . The “ 1σ ” allowed regions of Fig. 1 are collapsed to their central values, except for Δm_s which is a 95% CL limit boundary excluding the left region. The combined constraints on (ρ, η) are indicated by the 68 and 95% CL contours, and translate to $\sin(2\beta) = 0.75 \pm 0.09$ [5]. Superimposed is the CDF $\sin(2\beta)$ measurement with two of the four solutions for β shown (long dashed lines). The 1σ allowed range (light shaded region) is shown for the smaller β solution. Right: Summary of $\sin(2\beta)$ measurements [32, 33], Run II projections, and an indirect “ 1σ ” range reported at this Conference [6].

presentation from T. Miao, M. Paulini, C. Paus, F. Stichelbaut, and J. Tseng is appreciated.

References

- [1] N. Cabibbo, *Phys. Rev. Lett.* **10**, 531 (1963); M. Kobayashi and K. Maskawa, *Prog. Theor. Phys.* **49**, 652 (1973).
- [2] L. Wolfenstein, *Phys. Rev. Lett.* **51**, 1945 (1983).
- [3] UA1 Collaboration, C. Albajar et al., *Phys. Lett. B* **186**, 247 (1987).
- [4] ARGUS Collaboration, H. Albrecht et al., *Phys. Lett. B* **192**, 245 (1987).
- [5] S. Mele, CERN-EP/98-133, hep-ph/9810333.

- [6] A. Ali, *Proc. of the 13th Topical Conference on Hadron Collider Physics*, January 1999, Mumbai, India.
- [7] CDF Collaboration, F. Abe *et al*, *Nucl. Instrum. Methods A* **271**, 387 (1988); P. Azzi *et al*, *Nucl. Instrum. Methods A* **360**, 137 (1995).
- [8] DØ Collaboration, S. Abachi *et al*, *Nucl. Instrum. Methods A* **338**, 185 (1994).
- [9] S. Feher (DØ Collaboration), *Proc. of the 10th Topical Workshop on Proton-Antiproton Collider Physics*, Batavia, 1995, AIP Conf. Proc. Vol. 357, 1996.
- [10] CDF Collaboration, F. Abe *et al*, *Phys. Rev. D* **55**, 2546 (1997).
- [11] F. Bedeschi, (CDF Collaboration), *Proc. of the 10th Topical Workshop on Proton-Antiproton Collider Physics*, Batavia, 1995, AIP Conf. Proc. Vol. 357, 1996.
- [12] Particle Data Group, C. Caso *et al*, *Eur. Phys. J. C* **3**, 1 (1998).
- [13] DØ Collaboration, FERMILAB-Pub-96/357-E, 1996.
- [14] CDF Collaboration, F. Abe *et al*, FERMILAB-PUB-99/030-E.
- [15] T. Kuwabara, Ph.D. dissertation, University of Tsukuba, 1997.
- [16] S. C. Van Den Brink, Ph.D. dissertation, University of Pittsburgh, 1998.
- [17] CDF Collaboration, F. Abe *et al*, FERMILAB-PUB-99/019-E.
- [18] M. Gronau, A. Nippe, and J. Rosner, *Phys. Rev. D* **47**, 1988 (1993); M. Gronau and J. Rosner, *ibid.* **49**, 254 (1994).
- [19] D. Vucinic, Ph.D. dissertation, Massachusetts Institute of Technology, 1999.
- [20] CDF Collaboration, F. Abe *et al*, *Phys. Rev. Lett.* **80**, 2057 (1998).
- [21] CDF Collaboration, F. Abe *et al*, *Phys. Rev. D* **59**, 032001 (1999).
- [22] CDF Collaboration, F. Abe *et al*, FERMILAB-PUB-98/401-E.

- [23] H.-G. Moser and A. Roussarie, *Nucl. Instrum. Methods A* **384**, 491 (1997).
- [24] F. Parodi, *Proc. of XXIX International Conf. on High Energy Physics*, July 1998, Vancouver, B.C., Canada.
- [25] CDF Collaboration, F. Abe *et al*, *Phys. Rev. D* **59**, 032004 (1999).
- [26] M. Beneke, G. Buchalla, and I. Dunietz, *Phys. Rev. D* **54**, 4419 (1996).
- [27] J.H. Christenson *et al*, *Phys. Rev. Lett.* **13**, 138 (1964).
- [28] A. Riotto and M. Trodden, hep-ph/9901362, to be published in *Annual Review of Nuclear and Particle Science*, Vol. 49, December 1999.
- [29] CLEO Collaboration, J. Bartelt *et al*, *Phys. Rev. Lett.* **71**, 1680 (1993); OPAL Collaboration, K. Ackerstaff *et al*, *Z. Phys. C* **76**, 401 (1997); OPAL Collaboration, G. Abbiendi *et al*, CERN-EP/98-195.
- [30] A.B. Carter and A.I. Sanda, *Phys. Rev. Lett.* **45**, 952 (1980); I.I. Bigi and A.I. Sanda, *Nucl. Phys. B* **193**, 85 (1981).
- [31] S. Pappas (CDF Collaboration), *Proc. of DPF '99*, Jan 1999, Los Angeles, CA.
- [32] OPAL Collaboration, K. Ackerstaff *et al*, *Eur. Phys. J. C* **5**, 379 (1998).
- [33] CDF Collaboration, F. Abe *et al*, *Phys. Rev. Lett.* **81**, 5513 (1998).
- [34] Particle Data Group, R.M. Barnett *et al*, *Phys. Rev. D* **54**, 1 (1996).
- [35] G.J. Feldman and R.D. Cousins, *Phys. Rev. D* **57**, 3873 (1998).
- [36] CDFII Collaboration, FERMILAB-Pub-96/390-E, 1996.